THE JOURNAL OF BIOLOGICAL CHEMISTRY VOL. 284, NO. 31, pp. 20562–20573, July 31, 2009

Peptidoglycan Induces Cyclooxygenase-2 Expression in Macrophages by Activating the Neutral Sphingomyelinase-Ceramide Pathway*

Received for publication, June 2, 2009, and in revised form, June 12, 2009 Published, JBC Papers in Press, June 15, 2009, DOI 10.1074/jbc.M109.028084

Bing-Chang Chen[‡], Huey-Mei Chang[§], Ming-Jen Hsu[§¶], Chwen-Ming Shih[§‖], Yi-Hua Chiu[**], Wen-Ta Chiu[‡‡§§], and Chien-Huang Lin[§ §§¶¶1]

From the [‡]School of Respiratory Therapy, [§]Graduate Institute of Medical Sciences, Departments of [¶]Pharmacology and [‖]Biochemistry, and [‡‡]School of Medicine, College of Medicine, Taipei Medical University, Taipei 110, [**]Instrument Center, Office of Research and Development, Taipei Medical University, Taipei 110, the [§§]Taipei Medical University-Shuang Ho Hospital, Taipei County 235, and the [¶¶]Taipei Medical University-Wang Fang Hospital, Taipei 116, Taiwan

The sphingomyelin signal transduction pathway is known to play a role in mediating the action of various cytokines. Herein, we examined the role of neutral sphingomyelinase (nSMase)/ceramide in peptidoglycan (PGN)-induced NF-κB activation and cyclooxygenase-2 (COX-2) expression in macrophages. PGN-induced COX-2 expression was attenuated by an nSMase inhibitor (3-*O*-methyl-sphingomyeline, 3-OMS) and ceramidase, but not by an acidic SMase inhibitor (imipramine). C2-ceramide, bacterial SMase (which mimics cellular SMase activity), and a ceramidase inhibitor (*N*-oleoyl-ethanolamine) individually had no effect on COX-2 expression; however, they markedly enhanced PGN-induced COX-2 expression. PGN activated nSMase, but not acidic SMase, resulting in increased ceramide generation. PGN-induced nSMase activation and ceramide formation were inhibited by 3-OMS, but not by imipramine. PGN-induced COX-2 expression was inhibited by a p38 MAPK inhibitor (SB 203580) and dominant negative mutants of MAPK kinase (MKK) 3, MKK6, and p38 MAPKα. 3-OMS selectively inhibited PGN-induced p38 MAPK and MKK3/6 activation, but not JNK or ERK1/2. C2-ceramide, bacterial SMase, and *N*-oleoyl-ethanolamine all induced p38 MAPK or MKK3/6 activation. The PGN-mediated increases in κB-luciferase activity were also inhibited by 3-OMS and the p38 MAPKαDN, but not by imipramine. Furthermore, C2-ceramide caused an increase in κB-luciferase activity. Our data demonstrate for the first time that PGN activates the nSMase/ceramide pathway to induce MKK3/6/p38 MAPK activation, which in turn initiates NF-κB activation and ultimately induces COX-2 expression in macrophages. The nSMase/ceramide pathway is required but might not be sufficient for COX-2 expression induced by PGN.

Staphylococcus aureus is a major Gram-positive bacterial pathogen that activates the innate immune system of a host and induces the release of inflammatory molecules such as chemokines and cytokines (1–3). The bacterial cell wall components such as peptidoglycan (PGN)[2] and lipopolysaccharide, the main cell wall components of Gram-positive and -negative bacteria, respectively, can trigger an excessive release of proinflammatory cytokines (tumor necrosis factor α (TNF-α), interleukin (IL)-1, and IL-6) and chemokines (IL-8/CXCL8, macrophage inflammatory proteins 1 and 2, and monocyte chemoattractant protein) (4–6). These inflammatory molecules are the primary cause of most of the clinical manifestations of bacterial infections, including inflammation, fever, and septic shock (4–6). Notably, PGN constitutes ~90% of the cell wall components of Gram-positive bacteria (7), suggesting that PGN may play a critical role in the manifestations of bacterial infection. Toll-like receptors (TLRs), which recognize the structure of microorganisms, are essential for innate immune signaling (8). TLR2 has been shown to be a main receptor recognizing PGN, and its activation in response to PGN induces activation of transcription factor NF-κB and induction of proinflammatory cytokines (9, 10). For TLR2 signaling, TLR2 utilizes adaptor proteins, such as MyD88, to activate IL-1 receptor-associated kinase. Then the activated IL-1 receptor-associated kinase dissociates MyD88 from the receptor, followed by association with TNF-associated factor 6. This triggers activation of NF-κB, which is required for induction of gene expression (11). In addition, extracellular signal-regulated kinase (ERK) is also activated in response to PGN, which leads to activation of NF-κB transcription factor (12). However, little is known about the signal transduction molecules or transcription factors that regulate the induction of cyclooxygenase-2 (COX-2) protein by PGN.

There are two isoforms of COX, named COX-1 and COX-2, which have been cloned and identified to have 60% homology in humans (13, 14). Although both isoforms are involved in the formation of prostaglandins (15), they are likely to have fundamentally different biological roles. COX-1 is a housekeeping enzyme, is constitutively expressed in most mammalian tissues,

* This work was supported by National Science Council of Taiwan Grant NSC 96-2320-B-038-029-MY3 and Center of Excellence for Clinical Trial and Research in Neurology and Neurosurgery Grant DOH-TD-B-111–002.

[1] To whom correspondence should be addressed: 250 Wu-Hsing St., Taipei 110, Taiwan. Tel.: 886-2-27361661, Ext. 7100; Fax: 886-2-27399145; E-mail: chlin@tmu.edu.tw.

[2] The abbreviations used are: PGN, peptidoglycan; 3-OMS, 3-*O*-methyl-sphingomyeline; aSMase, acidic sphingomyelinase; COX, cyclooxygenase; DN, dominant negative mutant; ERK, extracellular signal-regulated kinase; IKK, IκB kinase; IL, interleukin; JNK, c-Jun N-terminal kinase; MAPK, mitogen-activated protein kinase; MKK, MAPK kinase; nSMase, neutral sphingomyelinase; NOE, *N*-oleoyl-ethanolamine; PBS, phosphate-buffered saline; TNF, tumor necrosis factor; TLR, Toll-like receptor; PMSF, phenylmethylsulfonyl fluoride; HPLC, high pressure liquid chromatography; bSMase, bacterial sphingomyelinase.

and appears to be responsible for the production of prostaglandins that mediate normal physiological functions such as maintenance of the integrity of the gastric mucosa and regulation of renal blood flow. In contrast, COX-2 is considered to be an inducible immediate-early gene and can be rapidly and transiently induced by proinflammatory mediators, including endotoxins and cytokines (12, 16–18). COX-2 is thought to contribute to the generation of prostanoids at sites of inflammation (19).

Ceramide is an intracellular second messenger that can be generated by sphingomyelin membrane cleavage using either acid sphingomyelinases (aSMases) or neutral sphingomyelinases (nSMases) (20, 21). Increases in cellular ceramide have been reported in many cell types in response to a variety of stimuli. These include the inflammatory cytokines TNF and IL-1, as well as environmental stresses, such as UV light; differentiating agents, like vitamin D_3; and other immunomodulatory signals, including Fas and CD28 (22, 23). Accumulating evidence has linked ceramide to inflammation, immune responses, cell growth, differentiation, apoptosis, and many cellular signals that regulate gene transcription (23). A recent study from our laboratory showed that PGN induces TLR2, p85α, and Ras complex formation and subsequently activates the Ras/Raf-1/ERK pathway, which in turn initiates IκB kinase (IKK)α/β and NF-κB activation and ultimately induces COX-2 expression in RAW 264.7 macrophages (12). The purpose of this study was to identify the signaling pathway of PGN-induced ceramide formation and its roles in PGN-mediated NF-κB activation and COX-2 expression in macrophages. Our studies demonstrated that PGN might activate the nSMase/ceramide pathway to induce activation of the MKK3/6 and p38 MAPK pathway, which in turn initiates NF-κB activation and ultimately induces COX-2 expression in macrophages. The nSMase/ceramide pathway is required but might not be sufficient for COX-2 expression induced by PGN.

EXPERIMENTAL PROCEDURES

Materials—PGN (derived from *S. aureus*) was purchased from Fluka (Buchs, Switzerland). SB 203580 and diacylglycerol kinase were obtained from Calbiochem. C2-ceramide, C2-dihydroceramide, 3-*O*-methyl-sphingomyeline (3-OMS), and *N*-oleoyl-ethanolamine (NOE) were from Biomol (Plymouth Meeting, PA). C16:0 ceramide, C17:0 ceramide, C18:0 ceramide, C24:0 ceramide, and C24:1 ceramide were purchased from Avanti Polar Lipid, Inc. (Alabaster, AL). Recombinant mouse neutral ceramidase was purchased from R & D Systems (Minneapolis, MN). Dulbecco's modified Eagle's medium/Ham's F-12, fetal calf serum, and penicillin/streptomycin were purchased from Invitrogen. Antibodies specific for α-tubulin and COX-2 were purchased from Transduction Laboratories (Lexington, KY). Protein A/G beads, antibodies specific for ERK, ERK phosphorylated at Tyr^{204}, p38 MAPK, and anti-mouse and anti-rabbit IgG-conjugated horseradish peroxidase were purchased from Santa Cruz Biotechnology (Santa Cruz, CA). Antibodies specific for c-Jun N-terminal kinase (JNK) 1/2, JNK phosphorylated at Thr^{183}/Tyr^{185}, p38 MAPK phosphorylated at Thr^{180}/Tyr^{182}, and MAPK kinase (MKK) 3/6 phosphorylated at Ser^{189}/Ser^{207} were purchased from Cell Signaling (St. Louis, MO). Anti-mouse and anti-rabbit IgG-conjugated alkaline phosphatases were purchased from Jackson ImmunoResearch Laboratories (West Grove, PA). An Amplex Red sphingomyelinase assay kit was purchased from Invitrogen. A Ras dominant negative mutant (RasN17) was purchased from Upstate Biotechnology, Inc. (Lake Placid, NY). pGL2-ELAM-Luc (which is under the control of a single NF-κB binding site) and pBK-CMV-Lac Z were kindly provided by Dr. W.-W. Lin (National Taiwan University, Taipei, Taiwan). The MKK3 dominant negative mutant (MKK3DN), MKK6DN, and p38 MAPKαDN were kindly provided by Dr. C.-M. Teng (National Taiwan University, Taipei, Taiwan). [γ-^{32}P]ATP (6,000 Ci/mmol) was purchased from Amersham Biosciences. GenePORTER^{TM} 2 was purchased from Gene Therapy System (San Diego, CA). All of the materials for the SDS-PAGE were purchased from Bio-Rad. All other chemicals were obtained from Sigma.

Cell Culture—The mouse macrophage cell line RAW 264.7 was obtained from the American Type Culture Collection (Livingstone, MT), and the cells were maintained in Dulbecco's modified Eagle's medium/Ham's F-12 nutrient mixture containing 10% fetal calf serum, 100 units/ml of penicillin G, and 100 μg/ml streptomycin in a humidified 37 °C incubator. After reaching confluence, the cells were seeded onto either 6-cm dishes for immunoblotting or the kinase assays, 10-cm dishes for the ceramide formation assay, 3.5-cm dishes for the sphingomyelinase activity assay, or 12-well plates for transfection and the κB-luciferase assays.

Preparation of Primary Mouse Peritoneal Macrophages—Mouse-specific pathogen-free BALB/c mice, aged 6–8 weeks and weighing 20–25 g, were obtained from the National Laboratory Animal Center, National Applied Research Laboratory (Taipei, Taiwan) and maintained in a specific pathogen-free environment in the animal house of Taipei Medical University. The use of animals was approved by the Institutional Animal Care and Use Committee of Taipei Medical University. The peritoneal macrophages were prepared as described previously (24). BALB/c mice that had been intraperitoneally injected with 1.5 ml of 3% thioglycollate 3 days before macrophage isolation were ether-anesthetized with the peritoneal cavities lavaged with ice-cold 0.9% NaCl to remove elicited peritoneal macrophages and cultured at RPMI 1640 containing 10% fetal calf serum, 100 units/ml of penicillin G, and 100 μg/ml streptomycin in a humidified 37 °C incubator. The cells were cultured on 6-cm dishes for an immunoblotting assay.

Transfection and κB-Luciferase Assays—For these assays, 2×10^5 RAW 264.7 cells were seeded onto 12-well plates, and the cells were transfected the following day using GenePORTER^{TM} 2 with 0.5 μg of pGL2-ELAM-Luc and 0.5 μg of pBK-CMV-Lac Z. After 24 h, the medium was aspirated and replaced with fresh Dulbecco's modified Eagle's medium/Ham's F-12 containing 10% fetal calf serum and then stimulated with PGN (30 μg/ml) for another 24 h before being harvested. To assess the effects of nSMase and aSMase inhibitors, drugs were added to cells 20 min before PGN addition. To assay the effect of the p38 MAPKαDN, the cells were cotransfected with the p38 MAPKαDN, pGL2-ELAM-Luc, and pBK-CMV-Lac Z for 24 h and then treated with PGN. Luciferase activity was

determined using a luciferase assay system (Promega) and was normalized on the basis of Lac Z expression. The level of induction of luciferase activity was compared as a ratio of cells with and without stimulation.

Immunoblot Analysis—To determine the expressions of COX-2, α-tubulin, ERK phosphorylated at Tyr^{204}, ERK2, JNK phosphorylated at Thr^{183}/Tyr^{185}, JNK2, p38 MAPK phosphorylated at Thr^{180}/Tyr^{182}, p38 MAPK, and MKK3/6 phosphorylated at Ser^{189}/Ser^{207} in RAW 264.7 macrophages, proteins were extracted, and Western blotting analyses were performed as described previously (25). Briefly, RAW 264.7 macrophages were cultured in 6-cm dishes. After reaching confluence, the cells were treated with PGN or pretreated with specific inhibitors as indicated followed by PGN. After incubation, the cells were washed twice in ice-cold phosphate-buffered saline (PBS) and solubilized in extraction buffer containing 10 mM Tris (pH 7.0), 140 mM NaCl, 2 mM phenylmethylsulfonyl fluoride (PMSF), 5 mM dithiothreitol, 0.5% Nonidet P-40, 0.05 mM pepstatin A, and 0.2 mM leupeptin. Samples of equal amounts of protein (60 μg) were subjected to SDS-PAGE and then transferred onto a polyvinylidene difluoride membrane, which was then incubated in TBST buffer (150 mM NaCl, 20 mM Tris-HCl, and 0.02% Tween 20, pH 7.4) containing 5% nonfat milk. The proteins were visualized by specific primary antibodies and then incubated with horseradish peroxidase- or alkaline phosphatase-conjugated second antibodies. Immunoreactivity was detected using enhanced chemiluminescence following the manufacturer's instructions. Quantitative data were obtained using a computing densitometer with Image-Pro Plus image analysis software system (Eastman Kodak Co.).

Assay of Sphingomyelinase Activity—The activities of aSMase and nSMase were measured using an Amplex Red sphingomyelinase assay kit according to the procedures described by the manufacturer. Briefly, RAW 264.7 macrophages were cultured in 35-mm Petri dishes. After reaching confluence, the cells were treated with PGN (30 μg/ml) for the indicated time intervals or pretreated with specific inhibitors as indicated followed by PGN. After incubation, the cells were washed twice in ice-cold PBS and harvested. To assess aSMase activity, the cells were extracted in 1 ml of lysis buffer containing 50 mM sodium acetate (pH 5.0), 1% Triton X-100, 1 mg/ml aprotinin, 1 mM EDTA, and 100 μg PMSF for 30 min on ice. To assess nSMase activity, the cells were extracted in 1 ml of lysis buffer containing 0.1 M Tris-HCl, 10 mM $MgCl_2$, (pH 7.4), 1% Triton X-100, 1 μg/ml aprotinin, 1 mM EDTA, and 100 μg/ml PMSF for 30 min on ice. After centrifugation at 12,000 rpm for 30 min at 4 °C, the resulting supernatants were assayed following the manufacturer's instructions. The assay mixture contained the following components in a total volume of 200 μl: 100 μl of the enzyme source (150 μg), 2 units/ml horseradish peroxidase, 0.2 unit/ml choline oxidase, 8 units/ml alkaline phosphatase, and 0.5 μM sphingomyelin. Assay mixtures were incubated at 37 °C for 30 min, and the fluorescence was measured with a HIDEX (Turku, Finland) chameleon microplate reader with excitation at 563 nm and emission at 587 nm.

Quantification of Ceramide—The quantification of ceramide in RAW 264.7 macrophages was performed as described previously (26). RAW 264.7 macrophages were cultured in 10-cm dishes. After reaching confluence, the cells were treated with PGN for the indicated time intervals. After incubation, the cells were washed twice in ice-cold PBS and collected in 0.5 ml of PBS. The cells were centrifuged at 1,500 rpm and 4 °C for 5 min. The PBS supernatant was removed, and the cells were stored at −80 °C. The lipids were extracted with 500 μl of methanol after the addition of internal standards (C17:0 ceramide). The suspension was incubated at 25 °C with 30 min of shaking and then centrifuged at 25,000 rpm for 30 min at 25 °C. The supernatants were collected, and the extraction step was repeated. The combined organic phases of ceramide were assayed. The liquid-liquid extractions; the amounts of C16:0 ceramide, C18:0 ceramide, C24:0 ceramide, and C24:1 ceramide; and the internal standards were determined by liquid chromatography coupled with tandem mass spectrometry. Chromatographic separation was accomplished under gradient conditions using a Luna C18 column (150 × 2 mm ID, 5-μm particle size, and 10-nm pore size). The HPLC mobile phases consisted of water-formic acid (100:0.1, v/v) (A) and acetonitrile-tetrahydrofuran-formic acid (50:50:0.1, v/v/v) (B). A gradient program was used for the HPLC separation at a flow rate of 0.3 ml/min. The initial buffer composition was 60% (A)/40% (B) held for 0.6 min, then linearly changed to 0% (A)/100% (B) in 4.4 min and held for 5 min, and then linearly returned to 60% (A)/40% (B) in 0.5 min and held for an additional 5.5 min. Forty microliters of each sample were injected, and the total run time was 16 min. Tandem mass spectrometry analyses were performed on an API 4,000 triple quadrupole mass spectrometer with a Turbo V source (Applied Biosystems). Precursor-to-product ion transitions of m/z 536.8 → 280.5 for C16:0 ceramide, m/z 564.9 → 308.5 for C18:0 ceramide, m/z 646.9 → 390.8 for C24:1 ceramide, m/z 648.9 → 392.8 for C24:0 ceramide, and m/z 550.9 → 294.5 for C17:0 ceramide were used for multiple reactions monitoring with a dwell time of 15 ms. Concentrations of the calibration standards, quality controls, and unknowns were evaluated by Analyst software 1.4.2 (Applied Biosystems). The mean peak areas of the samples reconstructed with internal standards were compared with the mean peak area of 10 ng/ml internal standards in methanol. Total ceramide was calculated from the sum of C16:0, C18:0, C24:0, and C24:1 ceramide subspecies.

Lipid Extraction and Ceramide Measurement—The lipids were extracted according to the method established by Bligh and Dyer (27), and ceramide was quantified by the diacylglycerol kinase assay. In brief, RAW 264.7 macrophages were grown in 10-cm dishes. After reaching confluence, the cells were pretreated with specific inhibitors as indicated followed by PGN. After incubation, the cells were pelleted by centrifugation (1,500 rpm for 5 min), washed twice with ice-cold PBS, and extracted with 3 ml of chloroform:methanol (1:2, v/v). Lipids in the organic phase extract were dried under N_2. Ceramide contained in each sample was resuspended in a 100-μl reaction mixture containing β-octylglucoside/dioleoylphosphatidylgerol (7.5%: 2.5 mM), 50 μl of 2× buffer, 19.4 μl dilution buffer, 2 mM dithiothreitol, 3 μg of *Escherichia coli* diacylglycerol kinase, and 2 μCi of [γ-^{32}P]ATP (3,000 Ci/mmol). After 30 min at room temperature, the reaction was stopped by extraction of lipids with 1.5 ml of chloroform:methanol (1:2), 0.3 ml of H_2O, 0.5 ml of chloroform, and 0.5 ml of 1% $HClO_4$. The lower

organic phase was dried under N_2 and resolved at 40 μl of chloroform:methanol (4: 1). Ceramide 1-phosphate was resolved by thin layer chromatography on silica gel 60 plates (Whatman, Pittsburgh, PA) using a solvent system of chloroform:acetone:methanol:acetic acid:H_2O (10:4:3:2:1) and detected by autoradiography.

Immunoprecipitation and the p38 MAPK Kinase Assay—RAW 264.7 cells were grown in 6-cm dishes. After reaching confluence, the cells were treated with 30 μg/ml PGN for the indicated time intervals or pretreated with specific inhibitors as indicated followed by PGN. After incubation, the cells were washed twice with ice-cold PBS; lysed in 1 ml of lysis buffer containing 20 mM Tris-HCl (pH 7.5), 1 mM $MgCl_2$, 125 mM NaCl, 1% Triton X-100, 1 mM PMSF, 10 μg/ml leupeptin, 10 μg/ml aprotinin, 25 mM β-glycerophosphate, 50 mM NaF, and 100 μM sodium orthovanadate; and centrifuged. The supernatant was then immunoprecipitated with a polyclonal antibody against p38 MAPK in the presence of A/G-agarose beads overnight. The beads were washed three times with lysis buffer and two times with kinase buffer containing 20 mM HEPES (pH 7.4), 20 mM $MgCl_2$, and 2 mM dithiothreitol. The kinase reactions were performed by incubating immunoprecipitated beads with 20 μl of kinase buffer supplemented with 20 μM ATP and 3 μCi of [γ-^{32}P]ATP at 30 °C for 30 min. To assess p38 MAPK kinase activity, 50 μg/ml of myelin basic protein was added to serve as the substrate. The reaction mixtures were analyzed by 15% SDS-PAGE followed by autoradiography.

Statistical Analysis—The results are presented as the means ± S.E. from at least three independent experiments. One-way analysis of variance followed by, when appropriate, Bonferroni's multiple range test was used to determine the statistical significance of the difference between means. A p value of < 0.05 was considered statistically significant.

RESULTS

nSMase, but Not aSMase, Is Involved in PGN-induced COX-2 Expression—Previous study has found that PGN (1–100 μg/ml) induced COX-2 expression in a concentration-dependent manner, with a submaximal effect at 30 μg/ml (12). To explore whether nSMase and aSMase might mediate PGN-induced (30 μg/ml) COX-2 expression, the nSMase inhibitor, 3-OMS (28), and the aSMase inhibitor, imipramine (29), were used. As shown in Fig. 1*A*, pretreatment of RAW 264.7 macrophages with 3-OMS (3~30 μM) inhibited PGN-induced (30 μg/ml) COX-2 expression in a concentration-dependent manner. When cells were treated with 30 μM 3-OMS, PGN-induced COX-2 expression was inhibited by 61 ± 2% (n = 3). However, imipramine (3–30 μM) did not affect PGN-induced COX-2 expression (Fig. 1*A*). Next, we determined whether nSMase directly enhanced PGN-induced COX-2 expression. A lower concentration (3 μg/ml) of PGN was used in the following experiments. Treatment of RAW 264.7 macrophages with recombinant bSMase (0.1–0.3 unit/ml), an exogenous source of SMase that mimics SMase action by degrading membrane sphingomyelin to increase cellular ceramide levels (30, 31), did not induce COX-2 expression. However, treatment of cells with various concentrations (0.1, 0.2, and 0.3 unit/ml) of recombinant bacterial SMase concentration-

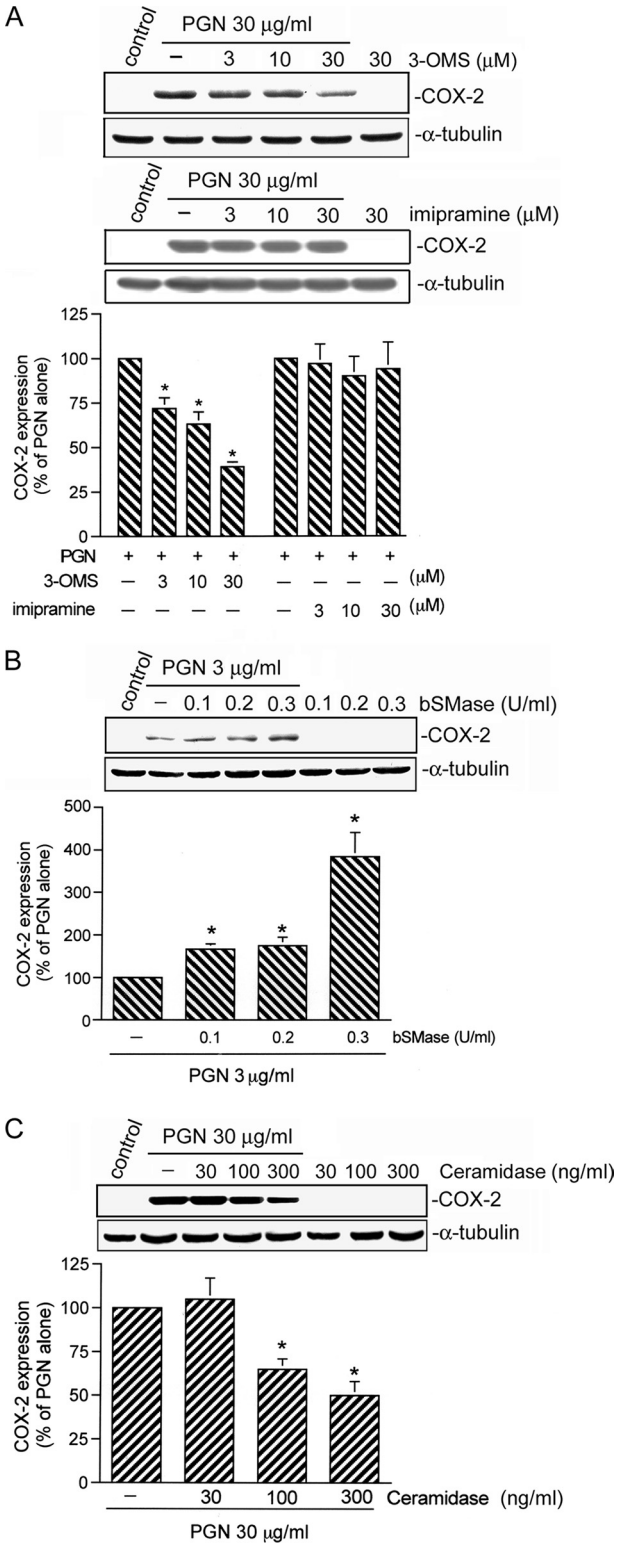

FIGURE 1. **Involvement of nSMase, but not aSMase, in PGN-induced COX-2 expression in RAW 264.7 macrophages.** *A*, cells were pretreated with various concentrations of 3-OMS or imipramine for 30 min before being incubated with PGN (30 μg/ml) for 24 h. *B*, cells were incubated with various concentrations of bSMase combined with PGN (3 μg/ml) for 24 h. *C*, cells were pretreated with ceramidase (30–300 ng/ml) for 30 min and incubated with PGN (30 μg/ml) for 24 h. Whole cell lysates were prepared and immunodetected with COX-2 or an α-tubulin-specific antibody. The presence of equal amounts of protein loading was confirmed by α-tubulin. The results shown are representative of three independent experiments. The results are expressed as the means ± S.E. *, $p < 0.05$, compared with the PGN-treated group.

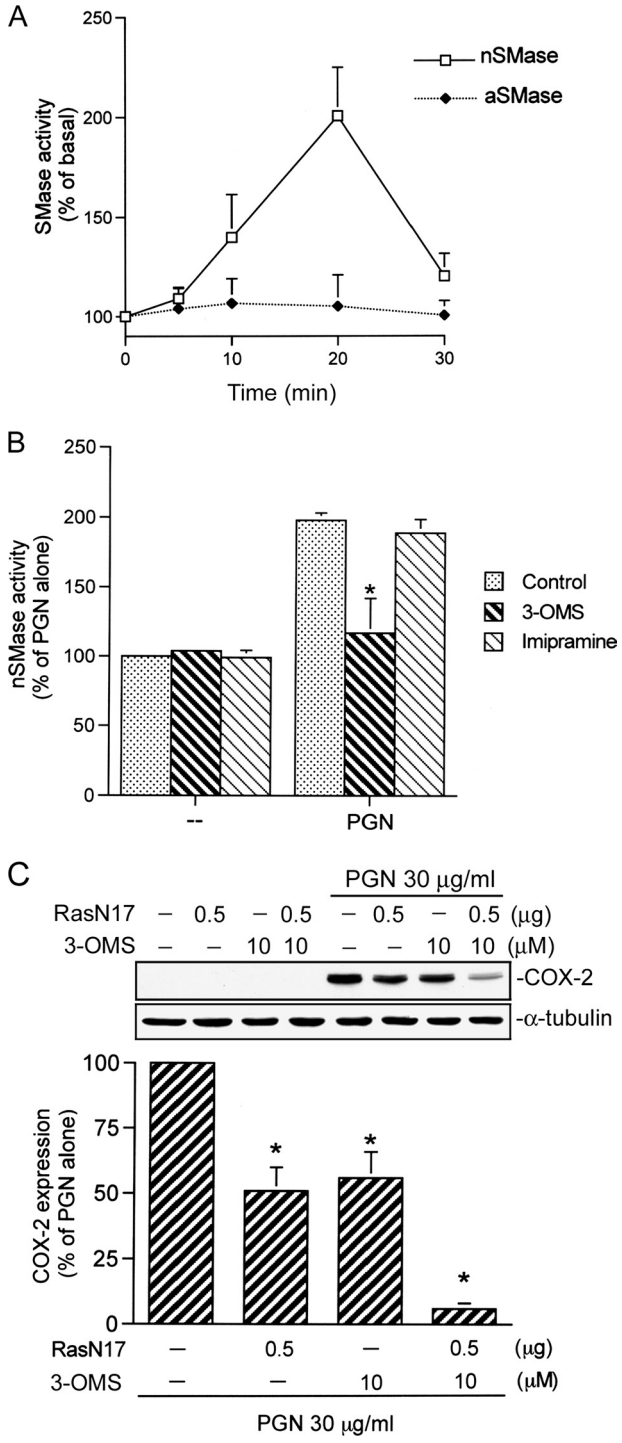

FIGURE 2. **PGN induced nSMase, but not aSMase, activation in RAW 264.7 macrophages.** *A*, cells were incubated with PGN (30 μg/ml) for the indicated time intervals. Whole cell lysates were prepared. The activities of nSMase and aSMase were measured as described under "Experimental Procedures." The results are representative of three independent experiments. *B*, cells were pretreated with 3-OMS (30 μM) and imipramine (30 μM) for 30 min and incubated with PGN (30 μg/ml) for another 20 min. After incubation, whole cell lysates were prepared. The nSMase activity was measured as described under "Experimental Procedures." The results are expressed as the means ± S.E. of three independent experiments performed in duplicate. *, $p < 0.05$, compared with the PGN alone group. *C*, cells were transfected with 0.5 μg of RasN17 for 24 h or pretreated with 10 μM 3-OMS for 30 min and then incubated with 30 μg/ml PGN for another 24 h. Whole cell lysates were prepared and immunodetected with COX-2 or an α-tubulin-specific antibody. The presence of equal amounts of protein loading was confirmed by α-tubulin. The results shown are representative of three independent experiments. The results are expressed as the means ± S.E. *, $p < 0.05$, compared with the PGN-treated group.

dependently enhanced COX-2 expression induced by the lower concentration (3 μg/ml) of PGN by 167 ± 12, 175 ± 20, and 385 ± 57%, respectively ($n = 3$) (Fig. 1*B*). Ceramide is metabolized by the ceramidase into sphingosin (26). We further explored whether ceramidase affected PGN-induced COX-2 expression. Treatment with macrophages with recombinant ceramidase (30–300 ng/ml) inhibited PGN-induced COX-2 expression in a concentration-dependent manner. When cells were treated with 300 ng/ml ceramidase, PGN-induced COX-2 expression was inhibited by 50 ± 8% ($n = 3$) (Fig. 1*C*). Next, we directly measured the activities of nSMase and aSMase induced by PGN stimulation in RAW 264.7 macrophages. Stimulation of cells with 30 μg/ml PGN induced an increase in nSMase activity in a time-dependent manner, reaching a maximum after 20 min of treatment (Fig. 2*A*). In contrast, PGN treatment did not alter aSMase activity (Fig. 2*A*). Confirming the effects of the nSMase inhibitors, a marked reduction in nSMase enzyme activity was observed in macrophages treated with 30 μM 3-OMS but not with 30 μM imipramine (Fig. 2*B*). These results suggest that nSMase, but not aSMase, is involved in COX-2 expression induced by PGN. Our previous study has shown that the Ras-dependent pathway is involved in PGN-induced COX-2 expression (12). Next, we investigated the relationship between the Ras and nSMase signal pathways involved in PGN-induced COX-2 expression. When cells were transfected with 0.5 μg of RasN17 and treated with 10 μM 3-OMS, they inhibited PGN-induced COX-2 expression by 49 ± 9 and 44 ± 10%, respectively (Fig. 2*C*). Furthermore, a combined treatment of cells with RasN17 and 3-OMS more markedly inhibited PGN-induced COX-2 expression by 87 ± 2% compared with RasN17 or 3-OMS alone (Fig. 2*C*). This result suggests that PGN-induced COX-2 expression occurs through the independent pathways of Ras and nSMase.

Ceramide Is Required but Might Not Be Sufficient for COX-2 Expression Induced by PGN—Ceramide is derived from sphingomyelin hydrolysis catalyzed by nSMase or aSMase (23). Treatment of cells with 30 μg/ml PGN increased ceramide formation. This response began at 20 min, peaked at 30 min, and sustained for 60 min. After 30 min of treatment, PGN (30 μg/ml) induced an increase in ceramide formation from 0.21 ± 0.02 to 0.46 ± 0.08 nmol/mg protein (Fig. 3*A*). We further examined whether ceramide is required for PGN-induced COX-2 expression. As shown in Fig. 3*B*, C2-ceramide (10–50 μM), a cell-permeable ceramide analogue, did not cause COX-2 expression, whereas it markedly potentiated PGN at the lower concentration-induced (3 μg/ml) COX-2 expression in a concentration-dependent manner by 220 ± 32, 363 ± 41, and 727 ± 134%, respectively ($n = 3$). C2-dihydroceramide, a cell-impermeable and inactive form of ceramide, did not enhance PGN-induced COX-2 expression at a concentration of up to 50 μM (Fig. 3*B*). NOE, a specific ceramidase inhibitor that prevents the degradation of cellular ceramide (32), did not result in COX-2 expression at a concentration of up to 50 μM. However, treatment of cells with various concentrations (10,

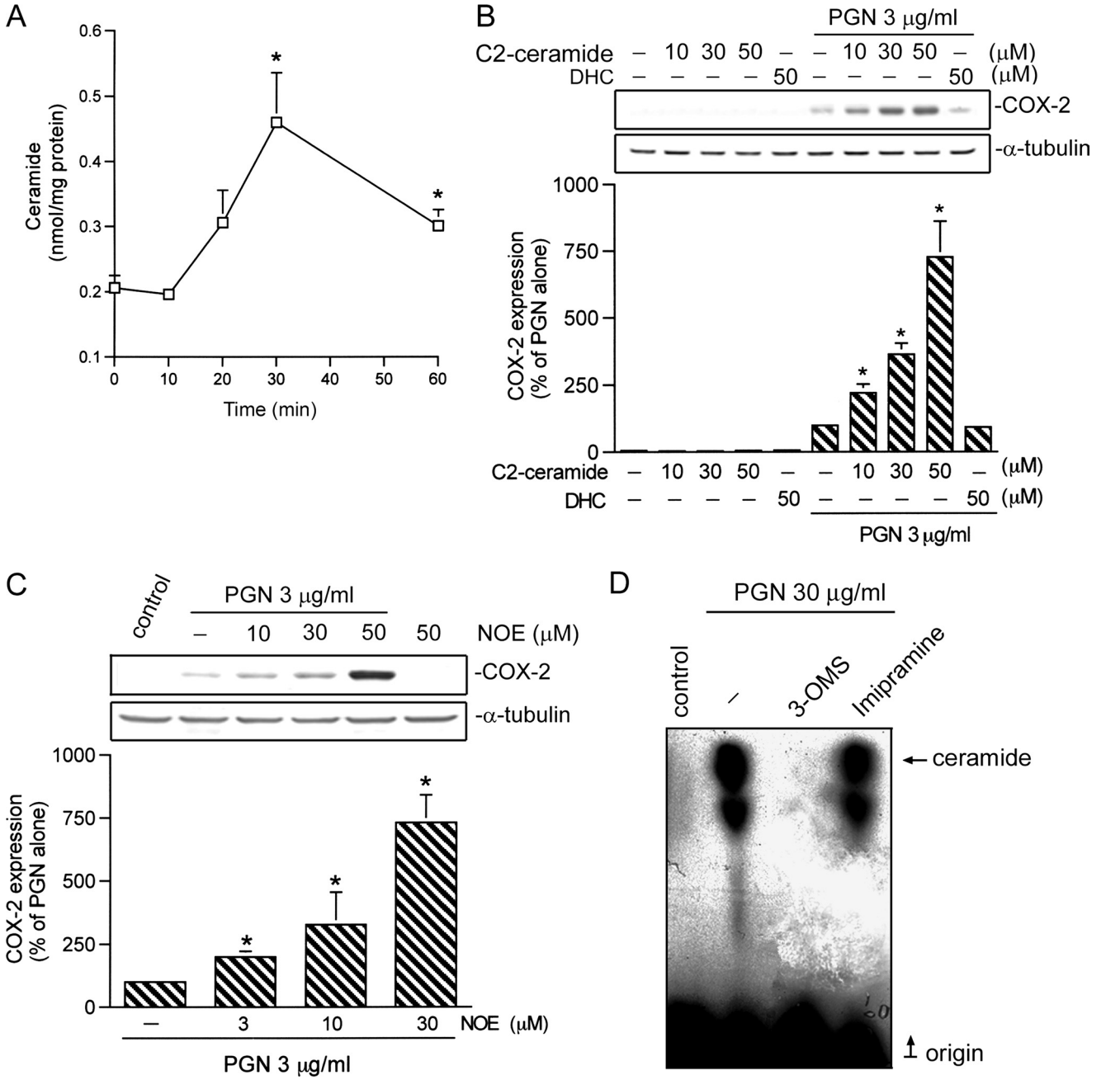

FIGURE 3. **Involvement of ceramide in PGN-induced COX-2 expression in RAW 264.7 macrophages.** *A*, cells were incubated with PGN (30 μg/ml) for the indicated time intervals. After lipid extraction, the ceramide formation in the extracts was measured using liquid chromatography coupled with tandem mass spectrometry as described under "Experimental Procedures." The results are expressed as the means ± S.E. of three independent experiments. *, $p < 0.05$, compared with the control group. *B*, cells were treated with various concentrations of C2-ceramide or 50 μM C2-dihydroceramide (*DHC*) combined with PGN (3 μg/ml) for 24 h. *C*, cells were treated with various concentrations of NOE combined with PGN (3 μg/ml) for 24 h. Whole cell lysates were prepared and immunodetected with COX-2 or an α-tubulin-specific antibody. The presence of equal amounts of protein loading was confirmed by α-tubulin. The results shown are representative of three independent experiments. The results are expressed as the means ± S.E. *, $p < 0.05$, compared with the PGN alone group. *D*, cells were pretreated with 3-OMS (30 μM) and imipramine (30 μM) for 30 min and incubated with PGN (30 μg/ml) for another 10 min. After lipid extraction, the ceramide in the extracts was measured using a diacylglycerol kinase assay and analyzed by thin layer chromatography as described under "Experimental Procedures." An *arrow* indicates the origin and ceramide. The results are expressed as the means ± S.E. of three independent experiments.

30, and 50 μM) of NOE concentration-dependently enhanced PGN-induced (3 μg/ml) COX-2 expression by 199 ± 8, 326 ± 129, and 732 ± 110%, respectively ($n = 3$) (Fig. 3*C*). PGN-induced ceramide formation was markedly attenuated by 3-OMS (30 μM) but not by imipramine (30 μM) (Fig. 3*D*). These results imply that the formation of ceramide is required but might not be sufficient for COX-2 expression induced by PGN.

MKK3/6 and p38 MAPK Are Involved in PGN-induced COX-2 Expression—To examine whether p38 MAPK might play a crucial role in PGN-induced COX-2 expression, the p38 MAPK inhibitor, SB 203580, was used. As shown in Fig. 4*A*, 1 μM of SB 203580 alone did not affect the basal COX-2 level, but it (0.1–1 μM) markedly inhibited PGN-induced (30 μg/ml) COX-2 expression in a concentration-dependent manner.

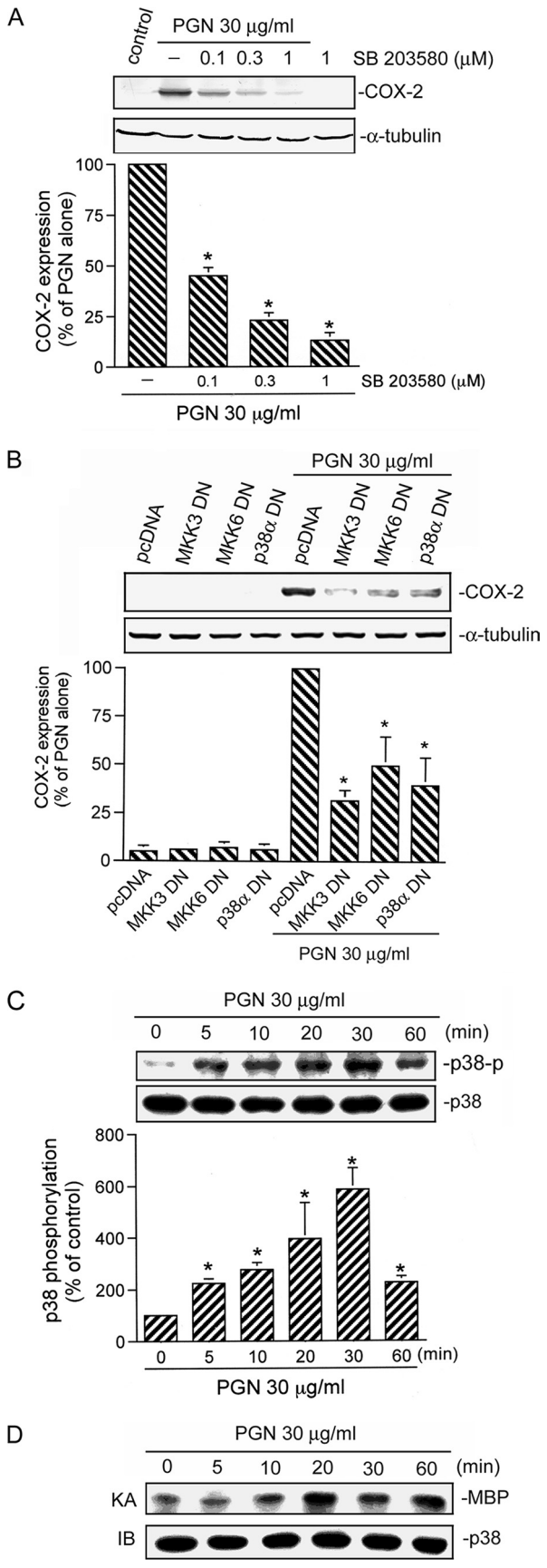

FIGURE 4. **Involvement of p38 MAPK and MKK3/6 in PGN-induced COX-2 expression in RAW 264.7 macrophages.** *A* and *B*, cells were pretreated for 30 min with various concentrations of SB 203580 (*A*) or transfected with the MKK3DN (1 μg), MKK6DN (1 μg), or p38 MAPKαDN (1 μg) (*B*) for 6 h and then stimulated with 30 μg/ml PGN for another 24 h. The cells were lysed and then immunoblotted for COX-2 or α-tubulin. Equal loading in each lane is demonstrated by the similar intensities of α-tubulin. The *traces* represent results from three independent experiments, which are presented as the means ± S.E. *, $p < 0.05$, compared with the PGN-treated group. *C*, cells were stimulated for the indicated time intervals with 30 μg/ml PGN for different intervals. The phosphorylation of p38 MAPK (*p38-p*) was measured in total cellular extracts by Western blotting with antibodies specific for phospho-p38 MAPK (*top panel*). The presence of equal amounts of the protein loading was confirmed by p38 MAPK (p38) (*bottom panel*). The results shown are representative of three independent experiments. The results are expressed as the means ± S.E. *, $p < 0.05$, compared with the control group. *D*, for p38 MAPK kinase activity, cell lysates were immunoprecipitated with a p38 MAPK antibody. One set of immunoprecipitates was subjected to a kinase assay (*KA*) using myelin basic protein as a substrate. The other set of immunoprecipitates was subjected to 12% SDS-PAGE and analyzed by immunoblotting (*IB*) with an anti-p38 MAPK antibody. Equal amounts of the immunoprecipitated kinase complexes present in each kinase assay were confirmed by immunoblotting for p38 MAPK. The data shown are representative of three independent experiments with similar results.

When cells were treated with 1 μM SB 203580, PGN-induced COX-2 expression was inhibited by 87 ± 4% ($n = 3$). To further confirm the role of the MKK3/6 and p38 MAPK signaling pathway in PGN-mediated COX-2 expression, MKK3DN, MKK6DN, and p38 MAPKαDN were tested. Transfection of RAW 264.7 cells individually with MKK3DN, MKK6DN, and p38 MAPKαDN all inhibited PGN-induced COX-2 expression by 68 ± 5, 50 ± 15, and 60 ± 14%, respectively ($n = 3$) (Fig. 4*B*). These results suggest that activations of MKK3/6 and p38 MAPK are required for PGN-induced COX-2 expression. Next, we directly measured the activation of p38 MAPK in response to PGN treatment. Fig. 4*C* shows that treatment of RAW 264.7 cells with 30 μg/ml PGN for various time intervals resulted in p38 MAPK activation, with an increase at 5 min and a maximum effect after 30 min of treatment. However, after 60 min of treatment with PGN, the response had decreased. In parallel, using myelin basic protein as a p38 MAPK substrate, an increase in p38 MAPK activity was observed within 10 min and reached a peak 20 min after PGN stimulation (Fig. 4*D*).

nSMase Is Involved in PGN-induced p38 MAPK, but Not ERK or JNK, Activation—Next, we identified which MAPKs are downstream of PGN-mediated nSMase activation. Pretreatment of RAW 264.7 macrophages for 30 min with 3-OMS (3–30 μM) inhibited PGN-induced p38 MAPK activation in a concentration-dependent manner (Fig. 5*A*). When cells were treated with 30 μM 3-OMS, PGN-induced p38 MAPK activation was inhibited by 67 ± 5% ($n = 3$) (Fig. 5*A*). However, it had no effect on PGN-induced JNK or ERK1/2 activation (Fig. 5, *B* and *C*). These results suggest that activation of p38 MAPK, but not JNK or ERK1/2, is downstream of PGN-induced nSMase activation. Furthermore, treatment of RAW 264.7 macrophages with 50 μM C2-ceramide induced p38 MAPK activation in a time-dependent manner, reaching a maximum after 30 min of treatment (Fig. 6*A*). Moreover, stimulation of cells with both bacterial SMase (0.3 unit/ml) and NOE (50 μM) also time-dependently induced p38 MAPK activation (Fig. 6, *B* and *C*).

nSMase/Ceramide Is Involved in PGN-induced MKK3/6 Activation—We next wished to determine whether PGN is able to activate MKK3/6, an upstream molecule of p38 MAPK (33). Treatment of cells with 30 μg/ml PGN caused MKK3/6 activation in a time-dependent manner. The PGN effect began at 10

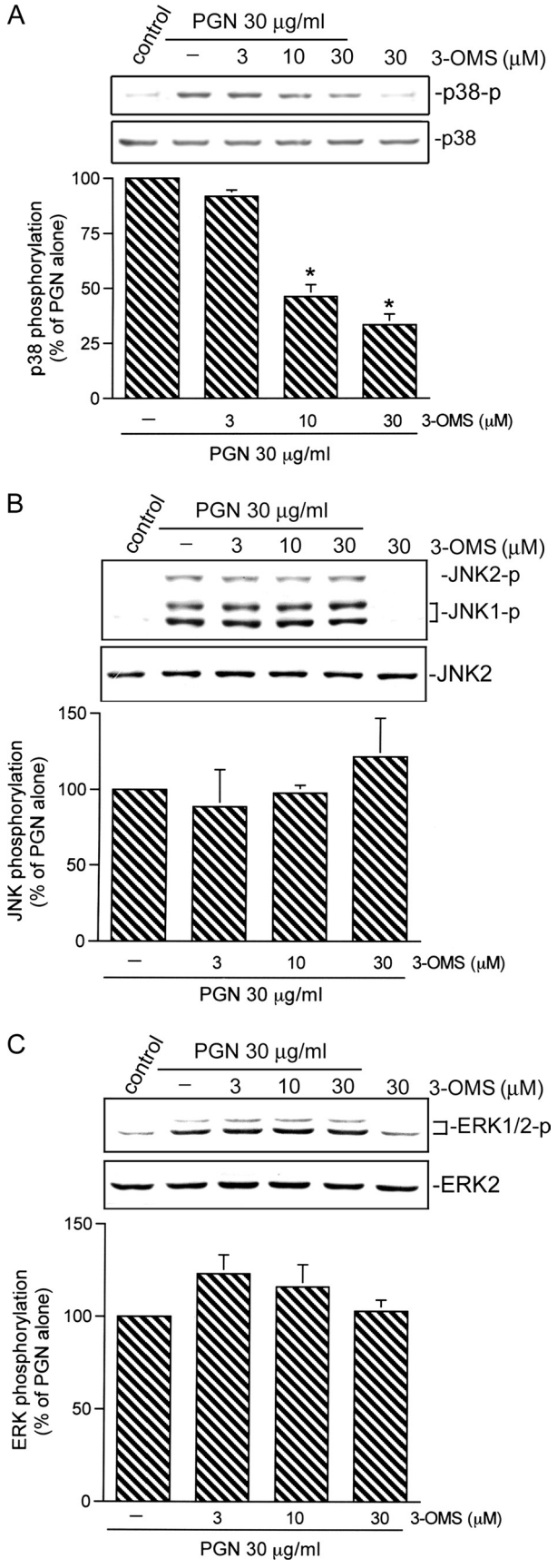

FIGURE 5. **Effects of an nSMase inhibitor (3-OMS) on PGN-induced p38 MAPK, JNK, and ERK1/2 activations in RAW 264.7 macrophages.** Cells were pretreated with various concentrations of 3-OMS for 30 min before being incubated with PGN (30 μg/ml) for another 30 min. The phosphorylations of p38 MAPK (*p38-p*) (*A*), JNK (*JNK-p*) (*B*), and ERK1/2 (*ERK1/2-p*) (*C*) in cell lysates were determined by immunoblotting with specific antibodies for phospho-p38 MAPK, phospho-JNK, and phospho-ERK1/2, respectively (*top panel*). Equal loading in each lane is indicated by the similar intensities of p38 MAPK, JNK2, and ERK2 (*bottom panel*). The results are expressed as the means ± S.E. *, $p < 0.05$, compared with the PGN alone group.

min and peaked at 30 min (Fig. 7*A*). We then further examined whether PGN-induced MKK3/6 activation occurs through nSMase/ceramide signaling pathways. As shown in Fig. 7*B*, pretreatment of RAW 264.7 macrophages with 3-OMS (3–30 μM) concentration-dependently inhibited PGN-induced MKK3/6 activation. When cells were treated with 30 μM 3-OMS, PGN-induced MKK3/6 activation was inhibited by 92 ± 4% ($n = 3$) (Fig. 7*B*). Moreover, stimulation of cells with 50 μM C2-ceramide also caused MKK3/6 activation, with an increase at 3 min and a maximum effect after 10 min of treatment. However, after 20 min of treatment with C2-ceramide, the response had decreased (Fig. 7*C*).

nSMase/Ceramide and p38 MAPK Mediated PGN-induced NF-κB Activation—We further examined whether activation of NF-κB occurs through the nSMase/ceramide/p38 MAPK signaling pathway. Using transient transfection with pGL2-ELAM-κB-luciferase as an indicator of NF-κB activity, we found that treatment of cells with 30 μg/ml PGN for 24 h caused an increase in κB-luciferase activity. The PGN-induced increase in κB-luciferase activity was markedly attenuated by 3-OMS (30 μM) by 40 ± 16% ($n = 3$), but not by imipramine (30 μM) (Fig. 8*A*). Transfection of RAW 264.7 cells with the p38 MAPKαDN also inhibited the PGN-induced increase in κB-luciferase activity by 72 ± 5% ($n = 3$) (Fig. 8*A*). Furthermore, treatment of cells with various concentrations of C2-ceramide also resulted in an increase in κB-luciferase activity in a concentration-dependent manner. After 24 h of treatment with 50 μM C2-ceramide, κB-luciferase activity had increased by ~204 ± 36% ($n = 3$) (Fig. 8*B*). Taken together, these data suggest that activation of the nSMase/ceramide/p38 MAPK pathway is required for PGN-induced NF-κB activation in RAW 264.7 macrophages.

nSMase, Ceramide, p38 MAPK, and NF-κB Mediated PGN-induced COX-2 Expression in Primary Mouse Peritoneal Macrophages—We further confirmed whether the nSMase/ceramide/p38 MAPK/NF-κB signal pathway is required for PGN-induced COX-2 expression in primary mouse peritoneal macrophages. As shown in Fig. 9*A*, ceramide (50 μM) potentiated PGN-induced COX-2 expression by 461 ± 55% ($n = 3$). The PGN-induced COX-2 expression was inhibited by 3-OMS (30 μM), SB 203580 (1 μM), and NF-κB inhibitor pyrrolidine dithiocarbamate (10 μM) by 49 ± 4, 49 ± 1, and 72 ± 7%, respectively (Fig. 9*B*). These results suggest that the nSMase/ceramide/p38 MAPK/NF-κB signal pathway is required for PGN-induced COX-2 expression in primary mouse peritoneal macrophages.

DISCUSSION

Recently, we found that PGN, a cell wall component of the Gram-positive bacterium *S. aureus*, may activate the Ras/Raf-1/ERK pathway, which in turn initiates IKKα/β and NF-κB activation and ultimately induces COX-2 expression in RAW

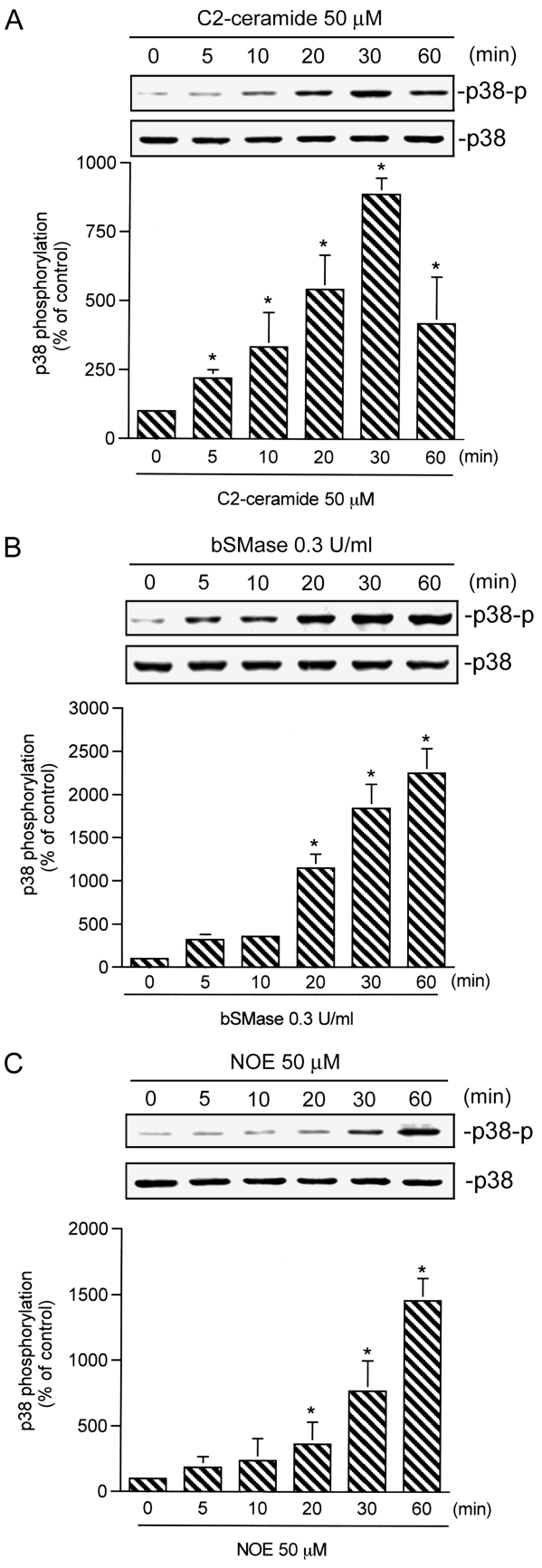

FIGURE 6. **Time-dependent stimulation of p38 MAPK activation by C2-ceramide, bSMase, and a ceramidase inhibitor (NOE) in RAW 264.7 macrophages.** Cells were stimulated with 50 μM C2-ceramide (*A*), 0.3 unit/ml bSMase (*B*), and 50 μM NOE (*C*) for the indicated time intervals. The phosphorylation of p38 MAPK (*p38-p*) was measured in total cellular extracts by Western blotting with an anti-phospho-p38 MAPK antibody. The presence of equal amounts of protein loading was confirmed by p38 MAPK (*p38*). The results shown are representative of three independent experiments. The results are expressed as the means ± S.E. *, $p < 0.05$, compared with the control group.

264.7 macrophages (12). Furthermore, we demonstrated that PGN-induced IL-6 production involves COX-2-generated prostaglandin E_2, EP2/EP4 receptor activation, intracellular cAMP formation, and the activations of cAMP-dependent protein kinase, protein kinase C, p38 MAPK, IKKα/β, p65 phosphorylation, and NF-κB (34). In the present report, we demonstrate that PGN might activate the nSMase/ceramide pathway to induce MKK3/6/p38 MAPK activation, which in turn initiates NF-κB activation and ultimately induces COX-2 expression in macrophages.

In this study, we found that PGN activated nSMase, but not aSMase, in RAW 264.7 macrophages. Additionally, the nSMase inhibitor prevented PGN-induced nSMase activation, ceramide generation, and COX-2 expression, whereas the aSMase inhibitor had no effect on these. Furthermore, bacterial SMase enhanced PGN-induced COX-2 expression. These results suggest that PGN-induced COX-2 expression is mediated via activation of nSMase leading to increased cellular ceramide generation. This suggestion is further supported by a previous report that found that TNF-α induces COX-2 expression via the nSMase signaling pathway in NCI-H292 epithelial cells (35). However, the signaling pathway involved in PGN-induced nSMase activation needs to be further investigated. A previous report indicated that $1,25(OH)_2D_3$-induced nSMase activation is mediated by protein kinase Cα in HL-60 cells (36).

In the present study, we found that treatment of RAW 264.7 macrophages with PGN caused the activation of MKK3/6 and p38 MAPK and that a p38 MAPK inhibitor (SB 203580) and dominant negative mutants of MKK3, MKK6, and p38 MAPKα all inhibited PGN-induced COX-2 expression. These results suggest that the MKK3/6/p38 MAPK signal pathway is very important for COX-2 induction caused by PGN. Our previous report also showed that p38 MAPK activation plays a critical role in lipoteichoic acid-mediated NF-κB activation and COX-2 expression in human airway epithelial cells (A549) (17). Previous studies showed that ceramide might activate ERK, JNK, and p38 MAPK (37, 38). However, in the present study, we found that an nSMase inhibitor (3-OMS) selectively inhibited PGN-induced p38 MAPK, but not ERK or JNK, activation. Moreover, C2-ceramide, bacterial SMase, and a ceramidase inhibitor (NOE) all caused p38 MAPK activation. These results suggest that activation of p38 MAPK, but not ERK and JNK, is downstream of PGN-induced nSMase/ceramide activation. This suggestion is further supported by a previous report that lipopolysaccharide induces COX-2 expression by activating sphingomyelinases leading to the release of ceramides, which in turn activate p38 MAPK, but not ERK, in rat microglia (39).

Recently, we showed that NF-κB activation contributes to PGN-induced COX-2 induction in RAW 264.7 macrophages (12). Furthermore, we also found that PGN may induce IKKα/β activation, IκBα phosphorylation, and IκBα degradation, as

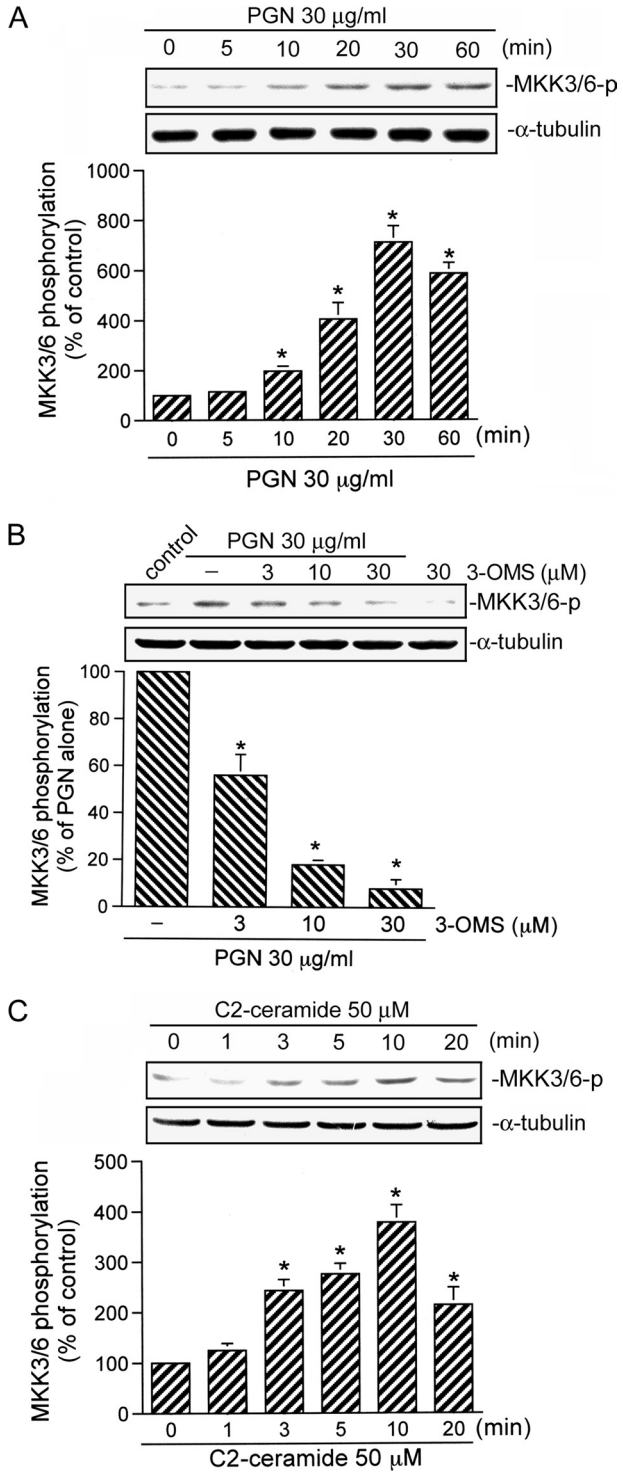

FIGURE 7. **PGN and C2-ceramide induced MKK3/6 activation and effects of nSMase inhibitor (3-OMS) on PGN-induced MKK3/6 activation in RAW 264.7 macrophages.** *A* and *C*, cells were treated with 30 μg/ml PGN (*A*) or 50 μM C2-ceramide (*C*) for different intervals, and MKK3/6 phosphorylation was determined by immunoblotting with an antibody specific for phosphorylated MKK3/6 (*MKK3/6-p*) (*top panel*). Equal loading in each lane is shown by the similar intensities of α-tubulin (*bottom panel*). Typical traces represent three experiments with similar results. *, $p < 0.05$, compared with the control group. *B*, cells were pretreated with various concentrations of 3-OMS for 30 min before being incubated with PGN (30 μg/ml) for another 30 min. The phosphorylation of MKK3/6 (MKK3/6-p) (*top panel*) in cell lysates was determined by immunoblotting with a specific antibody. Equal loading in each lane is shown by the similar intensities of α-tubulin (*bottom panel*). The results are expressed as the means ± S.E. *, $p < 0.05$, compared with the PGN alone group.

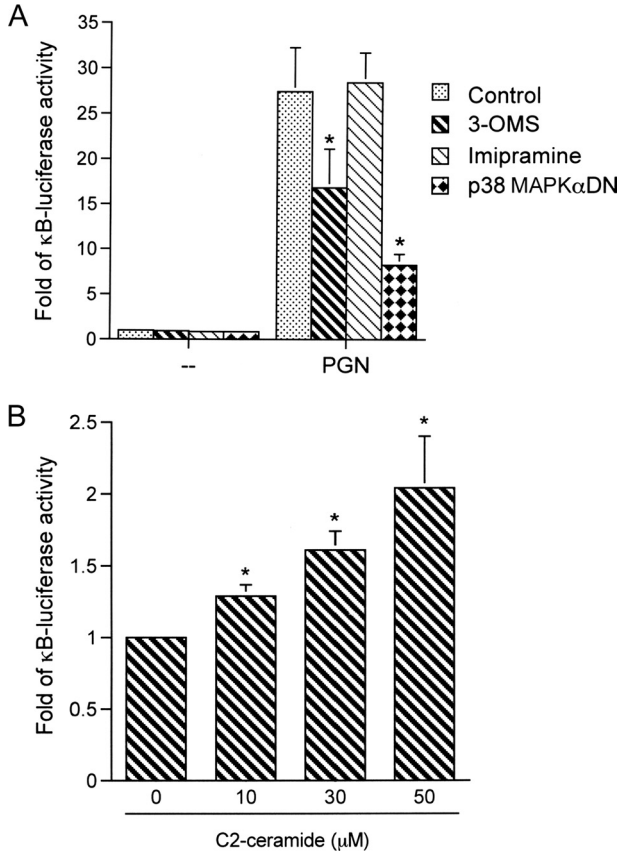

FIGURE 8. **Involvement of nSMase, C2-ceramide, and p38 MAPK in the PGN-induced increase in κB-luciferase activity in RAW 264.7 macrophages.** *A*, RAW 264.7 macrophages were transiently transfected with 0.5 μg of pGL2-ELAM-Luc and 0.5 μg of pBK-CMV-LacZ for 24 h, and the cells were pretreated with 3-OMS (30 μM) or imipramine (30 μM) for 30 min or transfected with p38 MAPKαDN (1 μg) for 6 h and then stimulated with PGN (30 μg/ml) for another 24 h. *B*, cells were transiently transfected with 0.5 μg of pGL2-EL-Luc and 0.5 μg of pBK-CMV-LacZ for 24 h and then treated with various concentrations (10–50 μM) of C2-ceramide for another 24 h. The cells were harvested for luciferase assay as described under "Experimental Procedures." The data represent the means ± S.E. of three experiments performed in duplicate. *, $p < 0.05$, compared with the PGN-treated group (*A*) or control group (*B*).

well as an increase in κB-luciferase activity (12). A previous report showed that in NCI-H292 epithelial cells, TNF-α leads to the activation of NF-κB through the nSMase signaling pathway (35). The p38 MAPK pathway also plays a critical role in NF-κB activation (39). As shown in Fig. 8, an nSMase inhibitor (3-OMS) and the p38 MAPKαDN blocked PGN-induced NF-κB reporter activity. Furthermore, C2-ceramide caused an increase in κB-luciferase activity. These results suggest that nSMase and ceramide are involved in PGN-mediated NF-κB activation through p38 MAPK activation.

In this study, we also found that 3-OMS (an nSMase inhibitor) inhibited PGN-induced (30 μg/ml) activations of MKK3/6, p38 MAPK, NF-κB, and COX-2 expression. Furthermore, we found that exogenous C2-ceramide induced the activations of MKK3/6, p38 MAPK, and NF-κB, whereas it did not induce COX-2 expression. Treatment of cells with C2-ceramide markedly potentiated a lower concentration (3 μg/ml) of PGN-induced COX-2 expression. Although bSMase and a ceramidase inhibitor (NOE) alone did not cause COX-2 expression, a combined treatment markedly potentiated PGN-induced COX-2

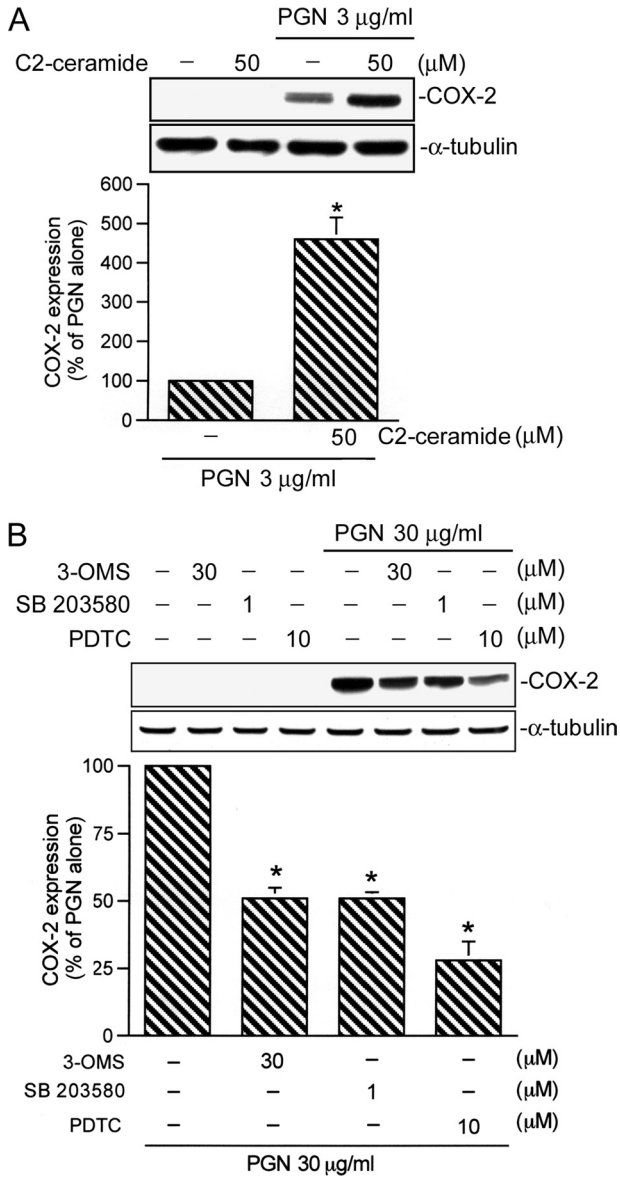

FIGURE 9. **Involvement of nSMase, C2-ceramide, p38 MAPK, and NF-κB in the PGN-induced COX-2 in primary mouse peritoneal macrophages.** *A*, mouse peritoneal macrophages were treated with 50 μM C2-ceramide combined with PGN (3 μg/ml) for 24 h. *B*, cells were pretreated with 3-OMS (30 μM), SB 203580 (1 μM), or pyrrolidine dithiocarbamate (*PDTC*, 10 μM) for 30 min and then stimulated with PGN (30 μg/ml) for 24 h. Whole cell lysates were prepared and immunodetected with COX-2 or an α-tubulin-specific antibody. The presence of equal amounts of protein loading was confirmed by α-tubulin. The results shown are representative of three independent experiments. The results are expressed as the means ± S.E. *, $p < 0.05$, compared with the PGN alone group.

expression. Based on these results, the formation of ceramide is required but might not be sufficient for PGN-induced COX-2 expression. This is consistent with the observation that C2-ceramide alone did not induce COX-2 expression but rather potentiated lipopolysaccharide-induced COX-2 expression in RAW 264.7 macrophages (40).

Recent studies indicated that ceramide is a bioactive lipid with the potential to regulate immune cell functions (41, 42). Ceramide is a well known intracellular second messenger and has been identified as a possible marker to predict multiorgan dysfunction in sepsis (42). Most ceramide species were increased in sepsis patients. In pathological conditions, the plasma ceramide concentration is ~10 μM (41). In this study, we found that exogenous C2-ceramide (10 μM) potentiated PGN-induced COX-2 expression. Previous studies showed that exogenous ceramide (10–50 μM) enhanced lipopolysaccharide- or IL-1β-induced COX-2 expression (40, 43). Therefore, ceramide plays an important role in enhancing inflammatory responses.

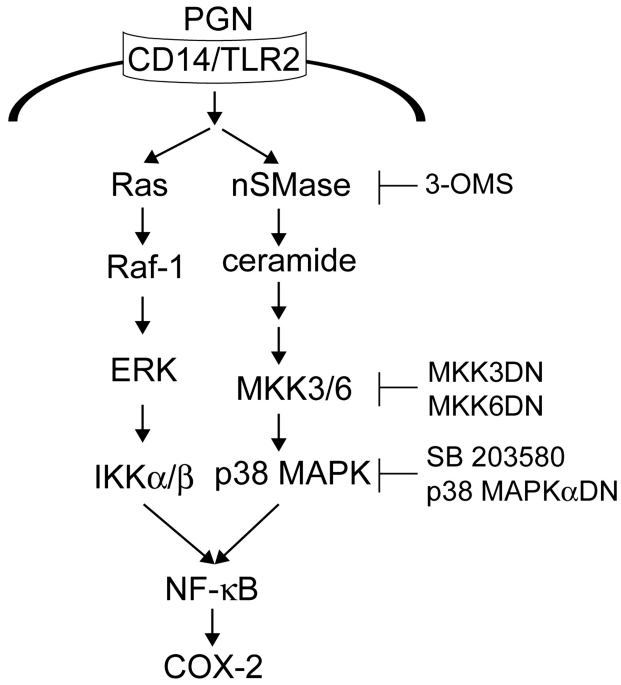

FIGURE 10. **Schematic diagram illustrating the proposed signaling pathway involved in PGN-induced COX-2 expression in macrophages through two separate pathways: the Ras/Raf-1/ERK pathway to induce IKKα/β activation and the nSMase/ceramide pathway to induce MKK3/6/p38 MAPK activation cascades resulting in an increase in NF-κB transactivation, ultimately causing COX-2 expression in macrophages.**

In conclusion, the findings of our study for the first time show that PGN might activate nSMase, but not aSMase, to induce ceramide formation, which in turn initiates MKK3/6, p38 MAPK, and NF-κB activation and ultimately induces COX-2 expression by macrophages. However, the nSMase/ceramide pathway is required but might not be sufficient for COX-2 expression induced by PGN. The present study, together with our previous report (12) delineates, in part, the signal transduction pathways of PGN-induced COX-2 expression. Fig. 10 is a schematic representation of the signaling pathway of PGN-induced COX-2 expression in macrophages. With an understanding of these signal transduction pathways, we can design therapeutic strategies to reduce inflammation caused by Gram-positive organisms.

Acknowledgments—We thank Dr. Wan-Wan Lin for the kind gift of the pGL2-ELAM-Luc and pBK-CMV-Lac Z plasmids. We also thank Dr. Che-Ming Teng for the kind gift of MKK3DN, MKK6DN, and p38 MAPKαDN plasmids.

REFERENCES

1. Krivan, H. C., Roberts, D. D., and Ginsburg, V. (1988) *Proc. Natl. Acad. Sci. U.S.A.* **85,** 6157–6161

2. Janeway, C. A., Jr., and Medzhitov, R. (2002) *Annu. Rev. Immunol.* **20,** 197–216
3. Ulevitch, R. J., and Tobias, P. S. (1995) *Annu. Rev. Immunol.* **13,** 437–457
4. Bone, R. C. (1994) *Arch. Intern. Med.* **154,** 26–34
5. Schleifer, K. H., and Kandler, O. (1972) *Bacteriol. Rev.* **36,** 407–477
6. Xu, Z., Dziarski, R., Wang, Q., Swartz, K., Sakamoto, K. M., and Gupta, D. (2001) *J. Immunol.* **167,** 6975–6982
7. Palaniyar, N., Nadesalingam, J., and Reid, K. B. (2002) *Immunobiology* **205,** 575–594
8. Akira, S., Uematsu, S., and Takeuchi, O. (2006) *Cell* **124,** 783–801
9. Wang, Q., Dziarski, R., Kirschning, C. J., Muzio, M., and Gupta, D. (2001) *Infect. Immun.* **69,** 2270–2276
10. Wang, Z. M., Liu, C., and Dziarski, R. (2000) *J. Biol. Chem.* **275,** 20260–20267
11. O'Neill, L. A., and Bowie, A. G. (2007) *Nat. Rev. Immunol.* **7,** 353–364
12. Chen, B. C., Chang, Y. S., Kang, J. C., Hsu, M. J., Sheu, J. R., Chen, T. L., Teng, C. M., and Lin, C. H. (2004) *J. Biol. Chem.* **279,** 20889–20897
13. Mitchell, J. A., Larkin, S., and Williams, T. J. (1995) *Biochem. Pharmacol.* **50,** 1535–1542
14. Xie, W. L., Chipman, J. G., Robertson, D. L., Erikson, R. L., and Simmons, D. L. (1991) *Proc. Natl. Acad. Sci. U.S.A.* **88,** 2692–2696
15. Marnett, L. J., Rowlinson, S. W., Goodwin, D. C., Kalgutkar, A. S., and Lanzo, C. A. (1999) *J. Biol. Chem.* **274,** 22903–22906
16. Samad, T. A., Moore, K. A., Sapirstein, A., Billet, S., Allchorne, A., Poole, S., Bonventre, J. V., and Woolf, C. J. (2001) *Nature* **410,** 471–475
17. Lin, C. H., Kuan, I. H., Lee, H. M., Lee, W. S., Sheu, J. R., Ho, Y. S., Wang, C. H., and Kuo, H. P. (2001) *Br. J. Pharmacol.* **134,** 543–552
18. Maier, J. A., Hla, T., and Maciag, T. (1990) *J. Biol. Chem.* **265,** 10805–10808
19. Williams, C. S., Mann, M., and DuBois, R. N. (1999) *Oncogene* **18,** 7908–7916
20. Hannun, Y. A. (1994) *J. Biol. Chem.* **269,** 3125–3128
21. Spiegel, S., Foster, D., and Kolesnick, R. (1996) *Curr. Opin. Cell Biol.* **8,** 159–167
22. Kolesnick, R., and Golde, D. W. (1994) *Cell* **77,** 325–328
23. Hannun, Y. A. (1996) *Science* **274,** 1855–1859
24. Chen, B. C., Hsieh, S. L., and Lin, W. W. (2001) *J. Leukocyte Biol.* **69,** 280–288
25. Chen, B. C., Yu, C. C., Lei, H. C., Chang, M. S., Hsu, M. J., Huang, C. L., Chen, M. C., Sheu, J. R., Chen, T. F., Chen, T. L., Inoue, H., and Lin, C. H. (2004) *J. Immunol.* **173,** 5219–5228
26. Schiffmann, S., Sandner, J., Schmidt, R., Birod, K., Wobst, I., Schmidt, H., Angioni, C., Geisslinger, G., and Grösch, S. (2009) *J. Lipid Res.* **50,** 32–40
27. Bligh, E. G., and Dyer, W. J. (1959) *Can J. Biochem. Physiol.* **37,** 911–917
28. Zeng, C., Lee, J. T., Chen, H., Chen, S., Hsu, C. Y., and Xu, J. (2005) *J. Neurochem.* **94,** 703–712
29. Albouz, S., Le Saux, F., Wenger, D., Hauw, J. J., and Baumann, N. (1986) *Life Sci.* **38,** 357–363
30. Zhang, P., Liu, B., Jenkins, G. M., Hannun, Y. A., and Obeid, L. M. (1997) *J. Biol. Chem.* **272,** 9609–9612
31. Tonnetti, L., Verí, M. C., Bonvini, E., and D'Adamio, L. (1999) *J. Exp. Med.* **189,** 1581–1589
32. Pahan, K., Sheikh, F. G., Khan, M., Namboodiri, A. M., and Singh, I. (1998) *J. Biol. Chem.* **273,** 2591–2600
33. Enslen, H., Raingeaud, J., and Davis, R. J. (1998) *J. Biol. Chem.* **273,** 1741–1748
34. Chen, B. C., Liao, C. C., Hsu, M. J., Liao, Y. T., Lin, C. C., Sheu, J. R., and Lin, C. H. (2006) *J. Immunol.* **177,** 681–693
35. Chen, C. C., Sun, Y. T., Chen, J. J., and Chang, Y. J. (2001) *Mol. Pharmacol.* **59,** 493–500
36. Marcinkowska, E., Wiedłocha, A., and Radzikowski, C. (1997) *Biochem. Biophys. Res. Commun.* **241,** 419–426
37. Subbaramaiah, K., Chung, W. J., and Dannenberg, A. J. (1998) *J. Biol. Chem.* **273,** 32943–32949
38. Chen, C. L., Lin, C. F., Chang, W. T., Huang, W. C., Teng, C. F., and Lin, Y. S. (2008) *Blood* **111,** 4365–4374
39. Akundi, R. S., Candelario-Jalil, E., Hess, S., Hüll, M., Lieb, K., Gebicke-Haerter, P. J., and Fiebich, B. L. (2005) *Glia* **51,** 199–208
40. Cho, Y. H., Lee, C. H., and Kim, S. G. (2003) *Mol. Pharmacol.* **63,** 512–523
41. Drobnik, W., Liebisch, G., Audebert, F. X., Frohlich, D., Gluck, T., Vogel, P., Rothe, G., and Schmitz, G. (2003) *J. Lipid Res.* **44,** 754–761
42. Delogu, G., Famularo, G., Amati, F., Signore, L., Antonucci, A., Trinchieri, V., Di Marzio, L., and Cifone, M. G. (1999) *Crit. Care Med.* **27,** 2413–2417
43. Kirtikara, K., Laulederkind, S. J., Raghow, R., Kanekura, T., and Ballou, L. R. (1998) *Mol. Cell Biochem.* **181,** 41–48